3D two scale X-FEM crack model with interfacial frictional contact: Application to fretting fatigue

Emilien Pierrès, Marie-Christine Baietto, Anthony Gravouil, Guillermo Morales Espejel

3D two scale X-FEM crack model with interfacial frictional contact: Application to fretting fatigue

E. Pierres [a,*], M.C. Baietto [a], A. Gravouil [a], G. Morales-Espejel [a,b]

[a] LaMCoS, CNRS UMR 5259, Villeurbanne, France
[b] SKF Engineering and Research Centre, Nieuwegein, The Netherlands

A global approach coupling experiments and numerical modeling is proposed to enhance crack prediction. Fretting tests have been conducted under conditions leading to crack formation. Three dimensional crack shapes have been reconstructed from metallographic cross-sections and described with level set functions. They are then used as input data in 3D two-scale X-FEM model detailed in this paper. Frictional contact conditions holding between the crack faces are accounting for. The methodology developed to describe those contact conditions at the pertinent scale is detailed.

A 3D fretting fatigue test is modeled to illustrate the coupling between experiments and numerical modeling.

1. Introduction

Fretting has long been recognized as a source of wear and premature fatigue failure within mechanical parts. Fretting damage may occur whenever a junction between contacting parts is subjected to cyclic sliding micromotions, whose characteristic amplitudes are much less than the size of the contact. Numerous studies have shown that wear and cracking processes may coexist within the same contact [1,2]. The introduction of fretting map concept establishes a close link between the main initial fretting damage and the regime of the running conditions [3].

In the cracking domain, multiple surface breaking cracks located in the contact vicinity initiate at a very early stage and most of the component life incorporates crack growth. From an experimental point of view, the inability to localize, identify and monitor the nucleation and growth of cracks within the contact interface and hence the great lack of information regarding the crack shape evolution versus the number of cycles is certainly a factor impeding the development of reliable fretting models.

Fretting experiments using macroscopic model contacts between polymers and rigid counterfaces have, however, emerged as a route to capture the complexities of fretting damage [4,5]. In this context, the selection of appropriate brittle glassy polymers offers the possibility of performing a continuous in situ visualisation of the crack development processes within the loaded contact zone. When associated with photoelastic devices [6], these experiments can also provide a convenient way of identifying the complex sliding behavior of the crack faces during the fretting cycle.

For opaque materials, crack shapes are reconstructed owing to post-mortem cross sections and metallographic observations [7,8]. In the last years, some attempts have been carried out to follow continuously the crack propagation using X-ray tomography. The latter is a very attractive technique which enables the visualisation of internal features in a sample. Being a non-destructive technique, it also enables, in principle, in situ visualisation of damage during loading and provides therefore the chronology of damage initiation and growth [9,10]. Fretting crack characterization is not feasible under load. Buffière et al. [11] have in that context, first conducted fretting tests in order to initiate at least a small fretting crack in the slip zone of the fretting scar, before the fretting pre-cracked specimen was loaded and cycled using an in situ uni-axial fatigue testing machine during scans.

In addition to those experimental difficulties, the numerical simulation of such 3D fretting cracks is also complicated by the contradictory constraints that must be met to successfully address this problem. The first one is that the problem is strongly multi-scale. Dimensions ranging from the meter (characteristic size of a component), to the mm (two-body contact patch, crack) and the μm (frictional contact zone at the crack interface) are encountered. Fretting cracks are then further submitted to multi-axial non-proportional and severe stress gradients and experienced complex frictional contact sequences at their interface. This local contact and notably the history of tangential contact

* Corresponding author. Tel.: +33 4 72 43 64 89.
E-mail address: emilien.pierres@insa-lyon.fr (E. Pierres).

conditions between the crack faces have a great influence over the global behavior of the cracks [12,4]. An accurate description and solution of the frictional contact between the crack faces is an essential pre-requisite to determine the crack behavior.

The eXtended Finite Element Method (X-FEM) is very well suited to 3D crack growth simulations. It is an extension of the finite element method based on the partition of unity and was introduced by Moës et al. [13]. The classical FEM bases of shape functions are enriched with discontinuous and asymptotic functions to capture the interface discontinuity and the asymptotic behavior close to the crack front. These enrichments avoid the mesh dependence of the initial crack shape. Thus, re-meshing and field interpolation are not required during the possible crack propagation. The method was extended and modified with an additional level set technique to handle arbitrary three-dimensional non-planar cracks [14–17]. The level set method is very efficient and robust to define the local enrichments associated to the crack and to update the three-dimensional crack geometry during its possible propagation. X-FEM has been applied to non-linear fracture mechanic quasi-static or dynamic problems [18–20]. X-FEM models accounting for contact along the crack faces have also been developed in two dimensions for static loadings [21–23]. Quasi-static models have also been proposed to describe fatigue crack growth simulation with frictional contact [24,25] and fatigue crack growth with unilateral contact and confined plasticity [26]. Lately, three-dimensional X-FEM models with frictional contact were addressed under static loading by Géniaut et al. [27].

The different scales involved within a structural or a fretting problem – i.e. those of the structure, of the crack and of possible localized non-linearities like confined plasticity or interfacial unilateral contact or frictional contact – differ by several orders of magnitude and an arbitrary finite element mesh of a given structure is usually not designed to account for a crack [28]. To overcome this drawback, the development of multi-scale strategies coupled with X-FEM is required. Recently X-FEM was combined with locally refined multi-grid (LMG-X-FEM) techniques for solving large 3D crack problems [29] without accounting for frictional contact at the crack interface. The scales of the crack and those of the structure are now gathered. Comparisons between 3D numerical crack modeling and 3D actual experimental crack patterns have been performed based on the combination of several procedures. Starting from experimental estimates of the crack pattern obtained either by micro-tomography and 3D Digital Image Correlation [30], or confocal scanning microscope observation [31], description of these actual crack patterns using levels set functions and X-FEM simulation based on the actual crack shape determination, is now feasible. Concerning frictional contact at crack interface, the necessity of a fine finite element mesh in the crack vicinity to capture at the pertinent scale the frictional non-linearities [25] was crude, even within two-dimensional X-FEM frictional fatigue crack framework. A two-scale strategy was proposed by Pierres et al. [32] to capture with a high efficiency in terms of CPU time and a great accuracy the contact effects at crack interface even with a coarse finite element mesh.

In this paper, the pre-cited two-scale X-FEM strategy [32] is extended to perform quasi-static fracture problem modeling with frictional contact along the crack faces, accounting for the history of the frictional contact conditions during fretting cycles. In Section 2, ball/plane fretting tests have been carried out under loading conditions inducing cracking as the main damage. The crack patterns are reconstructed thanks to post-mortem cross sections and metallographic observations. Section 3 is devoted to the presentation of the two-scale X-FEM strategy performed in the first place to analyze 3D unilateral crack problems [32] and here extended to 3D unilateral frictional contact fatigue crack problems. The fracture problem is divided into a global problem (defined by the structure and its relevant scales) and a local interface problem (formed by the crack faces and its own internal variables). The crack is considered as an autonomous entity with its own discretization scheme, variables and constitutive law [33] and is connected in a weak sense to the global problem. A formulation involving three fields is used. Furthermore, the accuracy of the contact solution depends on the discretization of the contact area, here formed by the crack faces. A new technique is developed to refine it independently of the mesh of the structure. The interface discretization is thus adapted to the frictional contact problem at the pertinent scale.

Numerical test cases are presented in Section 4 to illustrate the capacities and the performances of the model. Planar 3D cracks submitted to compressive loadings are considered. The frictional contact solution along the crack faces is compared to those obtained according to ANSYS modeling of the same configuration. The differences between both models in the mesh size and refinement are emphasized underlying the two-scale strategy efficiency.

Section 5 is concerned with a simplified modeling of the fretting test described in Section 2. The aim is to illustrate the coupling between experiments and numerical modeling. The crack patterns reconstructed from the metallographic observations are described by a level set modeling. A 3D two-scale X-FEM frictional contact fretting crack simulation is performed based on the previous actual crack shape determination.

2. Experimental fretting fatigue crack investigation

Three-dimensional ball/plane fretting fatigue tests are conducted under partial slip conditions leading to crack formation. Multiple surface breaking cracks located in the contact zone vicinity initiate at a very early stage. Generally only two of them, situated symmetrically from the centre of the contact zone, propagate whilst all the others are self-arrested. The two cracks propagate perpendicularly to the fretting direction, with a semi-elliptical shape at the surface for ball/plane configuration and may join each other at each edge of the specimen. For metallic materials, in situ continuous monitoring of such crack patterns is not feasible. At a number of cycles N, post-mortem successive cross-sections are performed and 3D crack shapes are reconstructed from information extracted from the successive 2D planar patterns. This process is lengthy and must moreover be performed for fretting tests carried out for different number of cycles to follow the crack shape evolutions.

A ball of radius $R=8.4$ mm is pressed against a plate of dimensions 24 mm × 16 mm × 4 mm with a static normal force $P=80$ N. A tangential sinusoidal cyclic displacement of amplitude $\delta x \approx 2$ μm is then imposed to the ball, cf. Fig. 1. The resulting

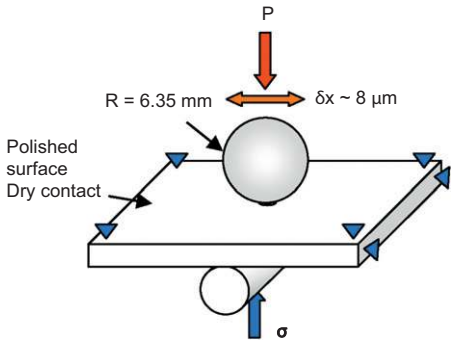

Fig. 1. Scheme of the experimental fretting test.

tangential force $Q=56$ N is recorded continuously during the test. Both contacting surfaces are polished and cleaned. The loading parameters (P, δ) have been chosen to produce partial slip at the two body interface within the elastic domain. In order to accelerate the crack initiation process, a static bending stress σ_s is superimposed to the planar sample. Tests are performed for different numbers of cycles ranging from 3000 to 200,000 cycles.

Accurate three dimensional data of the actual crack shapes extracted and reconstructed from different fretting tests performed for different number of cycles are obtained based on micro-metallographic observations. A fretting test carried out here for 70,000 cycles under controlled loading, was removed and cross sectioned. Observations at the ball/plane interface are displayed in Fig. 2(a). The central stick zone with the annulus slip zone are clearly visible, as well as the two cracks at the top surface. They initiate at both contact zone edges and extend perpendicularly to the fretting direction with a semi-elliptical shape. A cross section perpendicular to the surface is presented Fig. 2(b). 20 planar cross-sections have been performed successively to reconstruct a 3D crack pattern.

This procedure has been repeated for 30,000, 50,000 and 70,000 cycles to follow the contact and the crack shape evolutions. Note that the reproducibility of the tests regarding the crack initiation sites and paths allows this procedure. This is due to the highly localized stress–strain fields at the contact zone vicinity which are the mechanical driving mechanism for crack formation. The contact area with a top view of both cracks is displayed in Fig. 3(a) and the reconstruction of the crack pattern is

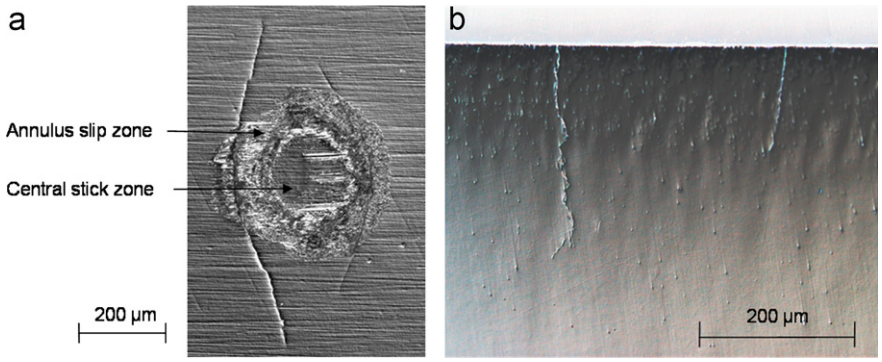

Fig. 2. (a) Cracked surface of the plane sample after 70,000 fretting cycles; and (b) one cross-section of the cracked volume.

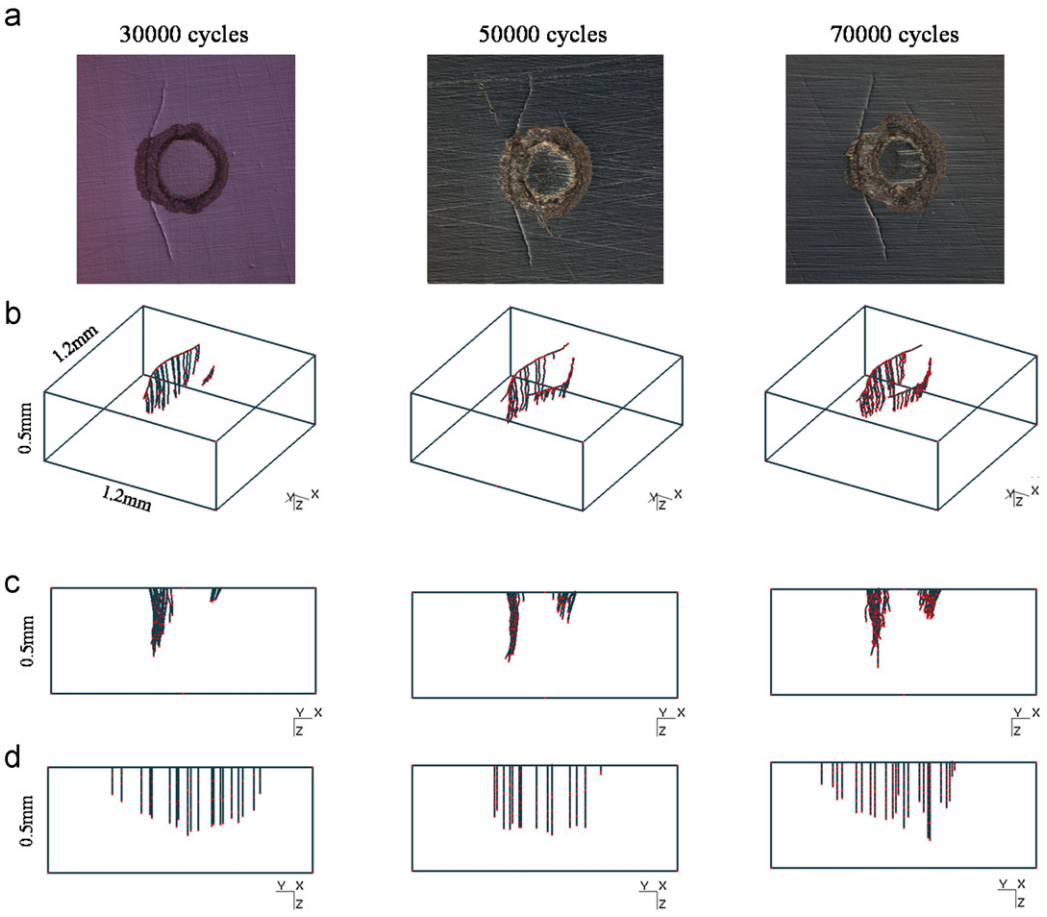

Fig. 3. Three-dimensional post-mortem reconstruction of the 3D fretting crack geometries using plane sections of the cracked sample submitted to 30,000, 50,000 and 70,000 fretting cycles (a) cracked contact surface; (b) reconstructed 3D crack shape; (c) projection on plane $y=0$; (d) projection on plane $x=0$.

plotted in Fig. 3(b), (c) ((*x*,*z*) view) and (d) ((*y*,*z*) view). 3D crack shapes are obtained. The resulting cracks are fairly symmetrical.

These cracks will be described with levels set functions in Section 5 and used as input data for the numerical modeling according to the two-scale X-FEM frictional contact fatigue crack model described in the next section.

3. Two scale X-FEM strategy for 3D crack growth simulation with interfacial frictional contact along the crack faces

3.1. Three field weak formulation of the fracture problem with frictional contact

Consider a 3D elastic body Ω subject to constraints and an external cyclic loading along its boundary. Let $\mathbf{u}$, $\boldsymbol{\sigma}$ and $\boldsymbol{\varepsilon}$ be, respectively, the displacement, stress and strain fields within Ω at a given time *t*. Let Γ_C be the crack surface and $\mathbf{n}_C$ its corresponding normal, with $\mathbf{w}$ and $\mathbf{t}$, respectively, the interface displacement and force fields. The frictional contact law dependent on the local contact status between the crack faces Γ_C^- and Γ_C^+ is expressed:

Let $\mathbf{n}_C$ and $\mathbf{n}_T$ be, respectively, the unit outward normal and tangential vectors to Γ_C^+. The contact force $\mathbf{t}^+$ and the displacement $\mathbf{w}^+$ along Γ_C^+ are expressed in the local frame attached to the crack ($\mathbf{t}^-$ and $\mathbf{w}^-$ along Γ_C^-, respectively) as follows:

$$\mathbf{w} = w_N\mathbf{n}_C + w_T\mathbf{n}_T \text{ and } \mathbf{t} = t_N\mathbf{n}_C + t_T\mathbf{n}_T \tag{3.1}$$

The opening and slip (relative displacements) at crack interface are defined as the evolution of the displacements between two points, one on each face of the crack, facing each other initially

$$[w_N] = w_N^+ w_N^- \text{ and } [w_T] = w_T^+ - w_T^- \tag{3.2}$$

The contact with friction conditions for $x \in \Gamma_C$ at a given time *t* are formulated with the Coulomb's friction law:

open zone:

$$[w_N(x,t)] > 0 \text{ and } t_N^+(x,t) = t_N^-(x,t) = 0 \tag{3.3}$$

contact zone:

$$[w_N(x,t)] = 0 \text{ and } t_N^+(x,t) = -t_N^-(x,t) \le 0$$
$$t_T^+(x,t) = -t_T^-(x,t) \tag{3.4}$$

stick zone:

$$\|t_T(\mathbf{x},t)\| < \mu_C\|t_N(\mathbf{x},t)\| \Rightarrow \Delta[w_T(\mathbf{x},t)] = 0 \tag{3.5}$$

slip zone:

$$\|t_T(\mathbf{x},t)\| = \mu_C\|t_N(\mathbf{x},t)\| \Rightarrow \exists\lambda > 0/\Delta[w_T(\mathbf{x},t)] = -\lambda t_T^+(\mathbf{x},t) \tag{3.6}$$

where μ_C is the friction coefficient between the crack faces and Δ corresponds to an increment of the considered quantity between two successive time steps $\boldsymbol{i}$. Indeed, the considered time interval $[0, T]$ equivalent to one fretting cycle is discretized with successive time steps $\boldsymbol{i}$ according to the oscillating fretting load during one cycle (fine time scale).

The proposed strategy considers the 3D cracked structure and the crack interface as two independent global and local problems [32] (cf. Fig. 4). These two problems are defined by their own set of equations and their own primal and dual variables. The global problem is associated to the quantities $(\mathbf{u}, \boldsymbol{\sigma})$. It satisfies the equilibrium equation in the bulk and obeys a constitutive law, possibly non-linear. The stress–strain law in the bulk between $\mathbf{u}$ and $\boldsymbol{\sigma}$ is here assumed to be elastic linear, homogeneous and isotropic. The solution must also fulfill Dirichlet and Neumann boundary conditions both on $\mathbf{u}$ and $\boldsymbol{\sigma}$. Concerning the local crack problem, it is associated to $(\mathbf{w}, \mathbf{t})$ quantities and obeys the local frictional contact. It is linked to the global problem in a weak sense in order to avoid possible instabilities in the contact solution [32]. A quasi-static $(\mathbf{u}, \mathbf{w}, \boldsymbol{\lambda})$ three-field weak formulation of the fracture problem at a given time *t* is proposed

$$\begin{cases} 0 = -\int_\Omega Tr[\boldsymbol{\sigma}(t)\boldsymbol{\varepsilon}(\mathbf{u}^*)]d\Omega + \int_{\Gamma_C}\boldsymbol{\lambda}(t)\cdot\mathbf{u}^* dS \\ \quad + \int_{\Gamma_C}[\mathbf{t}(t) - \boldsymbol{\lambda}(t)]\cdot\mathbf{w}^* dS \\ \quad + \int_{\Gamma_C}[\mathbf{u}(t) - \mathbf{w}(t)]\cdot\boldsymbol{\lambda}^* dS \end{cases} \tag{3.7}$$

$$\forall\mathbf{u}^* \in U_0^*, \forall\mathbf{w}^* \in W^*, \forall\boldsymbol{\lambda}^* \in \Lambda^*, \forall t \in [0,T]$$

where $\boldsymbol{\lambda}$ is the Lagrange multiplier field defined along the crack faces and U_0^*, W^*, Λ^* are the functional spaces of the virtual fields $\mathbf{u}^*$, $\mathbf{w}^*$ and $\boldsymbol{\lambda}^*$ with the good properties of regularity [32, 34].

The three-field weak formulation (3.7) is the basis for the X-FEM discretized two-scale formulation. Its main specificity lies in the weak link between the primal and dual variables of the bulk and the crack, ensured by the introduction of the Lagrange multiplier field $\boldsymbol{\lambda}$.

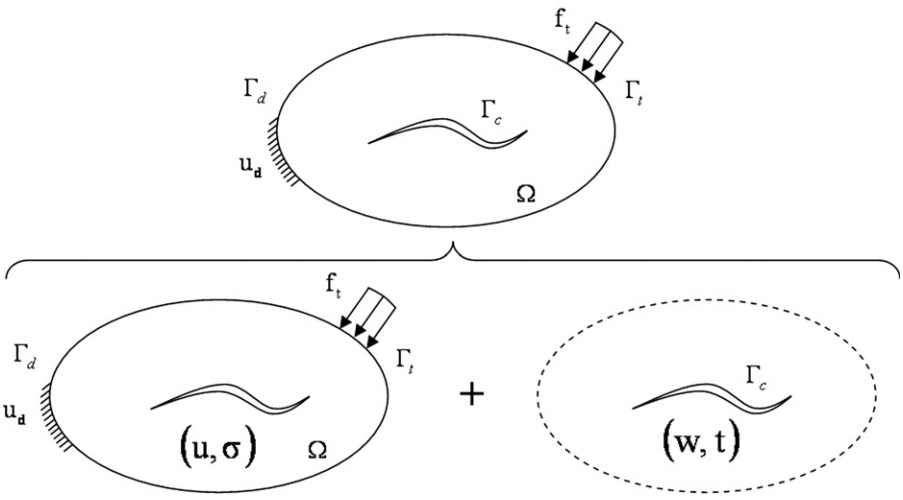

Fig. 4. Scheme and notations for the global and local fracture problems.

3.2. The eXtended Finite Element Method dedicated to frictional contacting crack

The eXtended Finite Element Method (X-FEM) is a very powerful technique to model crack and above all to perform crack growth simulation. Indeed, it enables the use of meshes not conforming to cracks. Further neither re-meshing nor field interpolation is needed during the possible crack propagation. This method is based on the Partition of Unity concept [35] and was introduced by Moës et al. [13]. The classical finite element bases of shape functions are enriched with discontinuous and asymptotic functions to account for the interface discontinuity and the asymptotic behavior at crack front crack, respectively (cf. Fig. 5). Furthermore, those specific local enrichments allow a good local accuracy close to the crack front even with rather coarse meshes compare to those employed with the finite element method (FEM). The X-FEM displacement field approximation $\mathbf{u}^h$ is

$$\mathbf{u}^h(\mathbf{x},t) = \sum_{i \in N_{nodes}} \mathbf{u}_i(t)\Phi_i(\mathbf{x}) + H(\mathbf{x}) \sum_{j \in N_{crack}} \mathbf{a}_j(t)\phi_j(\mathbf{x}) + \sum_{l=1}^{4} B_l \sum_{k \in N_{front}} \mathbf{b}_{lk}(t)\phi_k(\mathbf{x}) \tag{3.8}$$

where $\mathbf{u}_i$ is the standard finite element degrees of freedom, $\mathbf{a}_j$ is the degrees of freedom linked to the generalized Heaviside function H and $\mathbf{b}_{lk}$ is the degrees of freedom linked to the singular enrichment functions B_l of the crack front. ϕ_i is the linear shape functions basis of the 3D finite elements (order 1). A similar approximation is used for the virtual displacement field $\mathbf{u}^*$. This enriched displacement field is defined on the nodes of the initial given structure finite element mesh.

A set of two three-dimensional mesh-independent level set surfaces is used to define the crack geometry [14–17]. This level set method also allows a robust and accurate definition of the local enrichments associated to three-dimensional cracks and greatly facilitate the update of the crack geometry during the possible propagation [14,16]. This technique allows to deal with 3D complex actual crack geometries. The crack simulation is based on data extracted from tomographic images [36,30] or scanning electronic microscope [31] and described by levels set functions.

The numerical integration of the frictional contact law requires the discretization of the displacement and traction fields, w and t, respectively, as well as the Lagrange multiplier field λ. Interface elements have been introduced at the intersection between the X-FEM mesh and the crack geometry for tackling with 2D frictional contact crack within the X-FEM framework [21,25,26]. The crack discretization is hence dependent on the underlying finite element mesh, meaning that a local refinement of the finite element mesh around the crack required to get an accurate description of the frictional contact non-linearities between the crack faces implies a refinement of the finite element mesh. This strategy conflicts with the concept of crack/mesh independency inherent to X-FEM. Moreover, it is very laborious and CPU time consuming in 2D [25] and prohibitive in 3D. A two-scale strategy has been proposed for 3D unilateral contact crack within the X-FEM framework [32] to overcome this difficulty. A specific algorithm was proposed by Pierres et al. [32] to refine the interface discretization independently of the underlying finite element mesh. The linear interface elements are first created at the intersection between the crack geometry and the three dimensional X-FEM mesh as shown in Fig. 6. Quadrature Gauss points (G_i^+, G_i^-) connected to each interface element are defined on both faces of the crack. The crack interface fields $\mathbf{w}$, $\mathbf{t}$ and $\boldsymbol{\lambda}$ are calculated on the resulting distribution of Gauss points. The interface elements are then divided according to size and shape criteria as illustrated in Fig. 7. A uniform and refined distribution of the interface Gauss points adapted to the scale of the local frictional contact non-linearities is then obtained and allows capturing the contact/open distribution at a lower scale. Note that the weak formulation used here allows the use of incompatible discretizations and hence the Gauss point distribution at the interface does not need to match with the X-FEM mesh.

The following discretized linear system is derived from the weak formulation (3.7):

$$\begin{cases} \forall \mathbf{U}^* \Rightarrow \mathbf{F}_{int} \cdot \mathbf{U}(t) = \mathbf{F}_{ext} \cdot \mathbf{U}(t) + \mathbf{L}^T \boldsymbol{\Lambda}(t) \\ \forall \mathbf{W}^* \Rightarrow \mathbf{T}(t) - \boldsymbol{\Lambda}(t) = 0 \\ \forall \boldsymbol{\Lambda}^* \Rightarrow \mathbf{M}_1 \mathbf{U}(t) - \mathbf{M}_2 \mathbf{W}(t) = 0 \end{cases} \tag{3.9}$$

where $\mathbf{U}$, $\mathbf{W}$, $\mathbf{T}$ and $\boldsymbol{\Lambda}$ correspond to $\mathbf{u}$, $\mathbf{w}$, $\mathbf{t}$ and $\boldsymbol{\lambda}$ discretized fields, respectively; $\mathbf{M}_1$ and $\mathbf{M}_2$ are equivalent to "mortar" operators enabling the use of incompatible crack and bulk discretizations.

The next step is the solution of the problem defined in Section 3.1. The starting point was the work of Champaney et al. [37] who dealt with 2D cracks submitted to uni-axial loading. The iterative scheme used for the solution was based on the LATIN method (LArge Time INcrement method) [33]. The LATIN method consists in dividing the set of equations into two subsets, the local non-linear one (here the local equations of the frictional contact at the crack interface) and the linear global one (those of the structure). Ribeaucourt et al. [25] extended and modified this iterative solver to tackle successfully 2D cyclic incremental non-linear frictional contact problems at crack interface. Further, as the normal and tangential quantities, referring to both interface displacements and loads, are of different order of magnitudes, a specific indicator was proposed [25] to improve the convergence quality of the solution. This indicator is based on distinct normal and tangential local quantities ($\mathbf{w}$ and $\mathbf{t}$) instead of resting on a global one to assess the distance between two successive solutions given by the iterative solver. This iterative process and the modified indicator

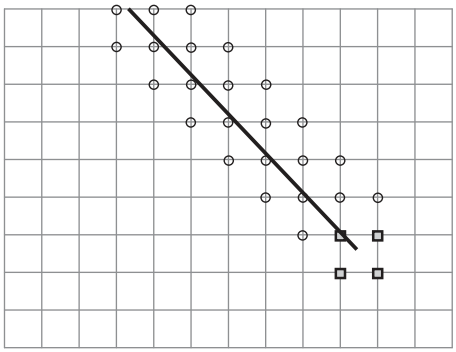

Fig. 5. Crack located on a regular mesh in two dimensions. X-FEM enriched nodes: squares for the local asymptotic enrichment and circles for the discontinuous local enrichments.

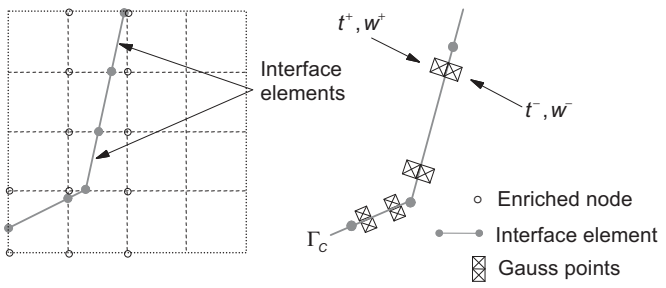

Fig. 6. Interface elements along crack profile with two Gauss points each.

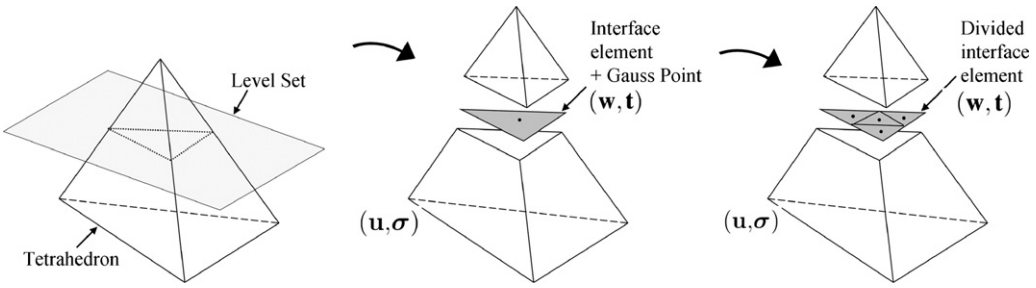

Fig. 7. Interface elements defined at the intersection between the level-set crack geometry and a 3D finite element. One Gauss point on each side per interface element.

are used here to solve the 3D unilateral and frictional contact problem within the X-FEM framework.

To conclude, the proposed two-scale X-FEM approach allows an intrinsic definition of the interface with its own primal variable (interface displacement field), its own dual variable (interface load field) and its own independent discretization adapted to the local non-linearities due to contact and friction at crack interface. A local refinement of the finite element mesh is hence not required. The 3D finite element mesh generation is simplified and complex contact states along the crack faces are captured at the pertinent scale for a low numerical cost [32]. Comparisons between 3D unilateral cracks submitted to compressive loadings have been performed. Fine and coarse finite element meshes were considered with or without using the two-scale strategy with interface refinement. Accurate results while obtaining very significant computer time reduction have been obtained for the coarse finite element mesh with interface refinement configuration compared to the finite element mesh configuration. However, if this finite element mesh is not fine enough to capture the global solution at a prescribed accuracy, the local contact solution will be affected, whatever the refinement of the crack discretization.

4. Numerical examples: validation of the 3D X-FEM model with frictional contact

Simple cases are now presented. The aims are to illustrate the capacities of the 3D two-scale X-FEM model with frictional contact at the crack interface and to compare the performances with those of existing industrial softwares. The first example considers a contacting and sticking crack, meaning that the crack does not influence the global solution and that the relative displacements between the crack faces [$\mathbf{w}(x, t)$] is nil. The second case considers a contacting partially sliding crack.

4.1. Contacting sticking cracks adherence problem

The cracked domain is a cube with 50 mm long edges. Young's modulus and Poisson's ratio are, respectively, equal to $E=200$ MPa and $\nu=0.3$. The surface breaking planar crack is inclined at an angle of 21.8° relatively to the plane $z=0$, with a straight front ($x=0$; $z=0$) as shown in Fig. 8(a). The bottom surface ($z=-25$ mm) is held fixed ($\mathbf{u}=0$). A vertical static compressive loading ($P=50$ MPa) is applied on the upper surface ($z=+25$ mm). A high friction coefficient at crack interface $\mu_C=1$ is chosen to induce sticking.

A rather coarse regular mesh of 3072 tetrahedra is considered, cf. Fig. 8(b). The proposed two-scale X-FEM model allows an intrinsic definition of the interface with its own discretization (distribution of interface Gauss points independent of the mesh in the bulk). The 360 Gauss point distribution over the interface elements (cf. Fig. 9(a)) obtained classically according to [21] is here refined as explained in Section 3.2. The interface is then discretized with 832 Gauss points as displayed in Fig. 9(b).

The approximation of the solution is computed at a level of accuracy of 10^{-4} using the local convergence criterion developed in [25]. Fig. 10(a) shows an amplified representation of the global displacement field **U** (norm of the global displacement vector $\times$ 250). The computed relative displacement field [**W**] is nil ($<5.10^{-7}$ m). A regular traction field **T** at the interface is plotted in Fig. 10(b). The mean value is equal to 50 MPa and is collinear to the Z-axis. Note that no traction field oscillation is observed. The global displacement solution is very close to the solution of a non-cracked body under an equivalent loading. However, small relative inaccuracy is observed in the vicinity of the crack front due to the use of standard X-FEM crack enrichments. Recent improvements like the treatment of blending elements or the use of new discontinuous enrichments can be adopted to palliate this difficulty.

The proposed 3D two-scale X-FEM model gives an accurate approximation of the global and local frictional contact solutions at a prescribed level of accuracy.

In the next example, 3D contacting stick/slip crack submitted to a compressive loading is simulated.

4.2. Contacting sliding cracks

The sample and the crack geometries, the material and the boundary conditions are identical to those considered in Section 4.1. A weak value of the friction coefficient between the crack faces $\mu_C=0.2$ is considered. The approximation of the solution is computed at a level of accuracy of 10^{-4} using the local convergence criterion developed in [25]. An amplified representation of the global displacement field **U**, the traction field **T** and the relative displacement field $[\mathbf{W}]=(\mathbf{W}^+-\mathbf{W}^-)$ at the interface obtained according to the proposed 3D two-scale X-FEM model are displayed in Fig. 11(a), (b) and (c), respectively. Regular local traction field and displacement fields are obtained.

As a reference, the numerical simulation of this example has been achieved using the finite element method software ANSYS. It is important to emphasize the great difference concerning the finite element meshes. The X-FEM one consists of 3072 elements (characteristic element size 5 mm) whereas in the ANSYS one 41,000 elements are used (element size from millimeter down to micrometer). A strong refinement is performed along the crack interface and especially in the front vicinity, it is clearly visible in Fig. 12(a) and (b). The comparison between the results obtained according to both models regarding the global displacement field **U** and traction field **T** at the crack interface are in a very good agreement. The same trends are observed. Further, very similar maximum values of **U** are obtained, 17 and 15 μm for X-FEM and ANSYS models, respectively.

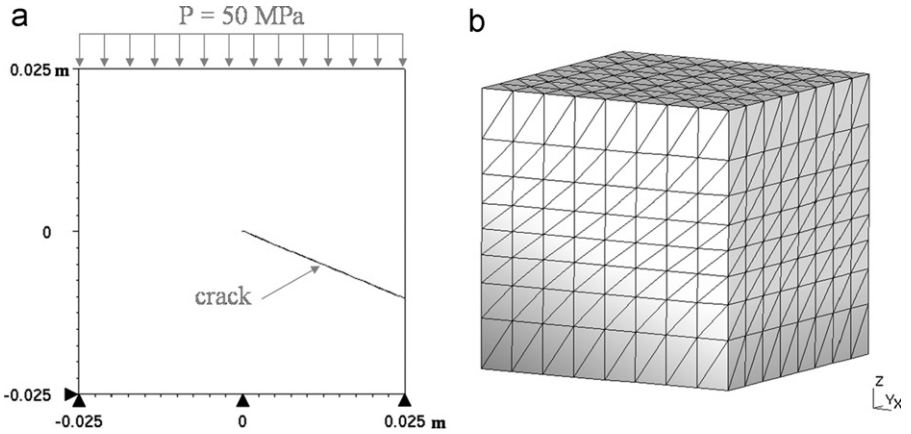

Fig. 8. (a) Geometry of the cracked problem (m), boundary and loading conditions and (b) regular X-FEM mesh non-conforming the crack: 3072 tetrahedra.

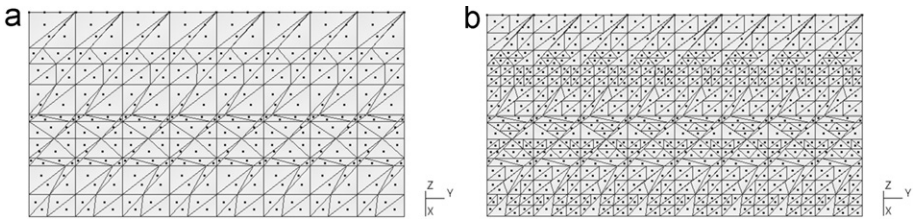

Fig. 9. Resulting interface elements with corresponding Gauss point distribution: (a) without refinement (360 Gauss points) and (b) with refinement (832 Gauss points).

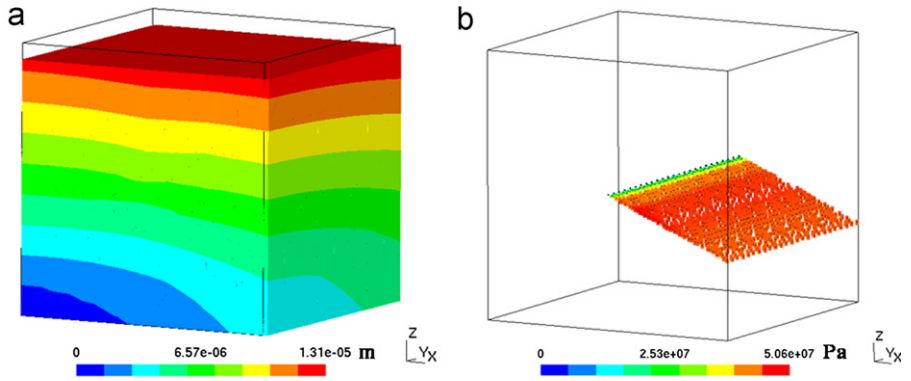

Fig. 10. 3D Two-scale X-FEM results for a friction coefficient $\mu_C=1$: (a) amplified representation of the global displacement field **U** ($\times 250$) and (b) traction field **T** at the interface.

This comparison highlights the quality of the frictional contact solution obtained according to the 3D two-scale X-FEM model using a coarse finite element mesh combined with an independent description of the local non-linearities at a pertinent scale. Significant savings in computing costs are moreover illustrated and will allow the analysis of large problems dealing with actual 3D crack patterns submitted further to cyclic frictional contact states.

The objectives of the numerical examples presented in this section were to validate by comparison and to illustrate the capacities of the proposed two-scale X-FEM model with frictional contact. The savings in computing costs have been further emphasized. In the next section, a more challenging configuration is simulated. Actual fretting crack patterns extracted and reconstructed from metallographic observations performed on post-mortem cross sections are described with level set functions. They are then used as input data for the fretting crack simulation according to the proposed two-scale X-FEM model.

5. 3D two-scale X-FEM simulation of an actual fretting crack pattern under simplified fretting loading

Sphere/plane fretting experimental tests have been carried out and analyzed regarding the crack patterns. The results have been detailed in Section 2. The objectives here are to describe those actual crack patterns with level set functions and to use those actual crack shapes as input data for the simulation of such 3D contacting frictional cracks during a fretting cycle based on the 3D two-scale X-FEM model.

The cracked sample is a regular parallelepiped of dimensions 8 mm $\times$ 5 mm $\times$ 2 mm. Boundary conditions $\mathbf{u}_z=0$ are defined on the bottom surface and the rigid body modes are fixed, cf. Fig. 13(a). Young's modulus and Poisson's ratio equal to $E=200$ MPa and $\nu=0.3$. The fretting tests carried out for 70,000 cycles are considered (cf. Fig. 2). The two elliptical surface breaking crack patterns are extracted and reconstructed from

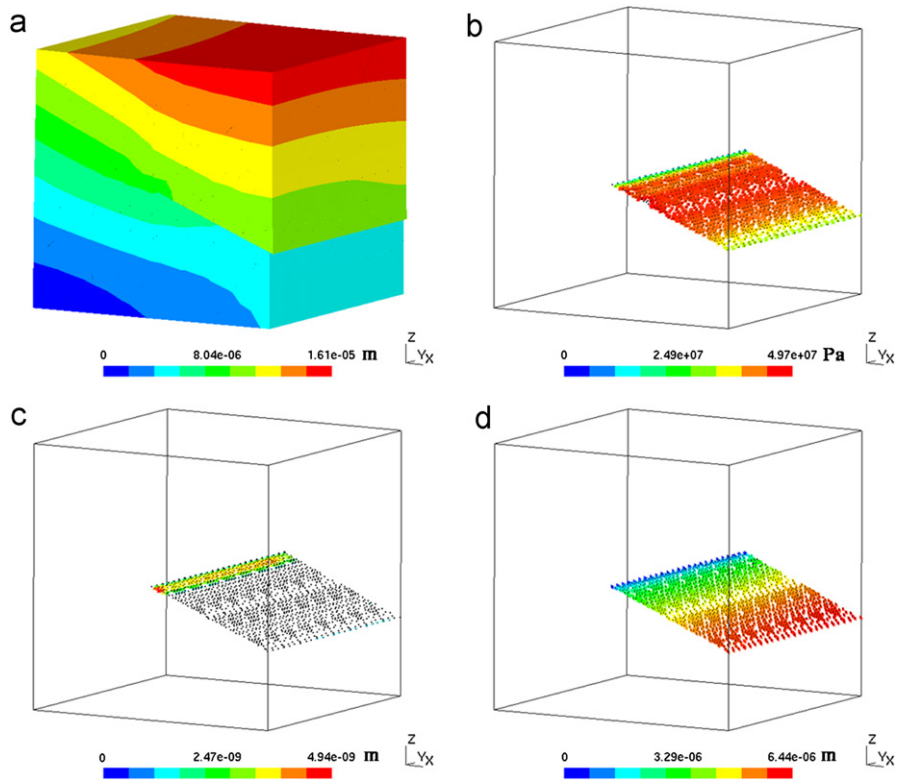

Fig. 11. Two-scale X-FEM results for a friction coefficient μ_C=0.2: (a) amplified representation of the global displacement field **U** (× 120); (b) traction field **T** at the interface; (c) relative normal displacement [$\mathbf{W_N}$] value at the interface; and (d) relative tangential displacement [$\mathbf{W_T}$] value at the interface.

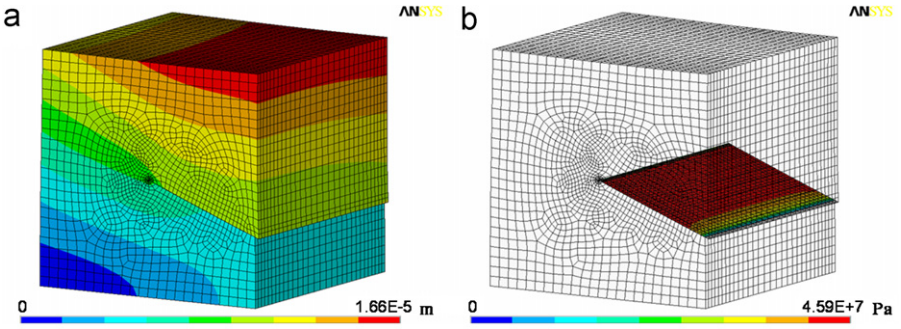

Fig. 12. ANSYS results for a friction coefficient μ_C=0.2: (a) amplified representation of the displacement field **U** (× 120) and (b) traction field **T** at the interface.

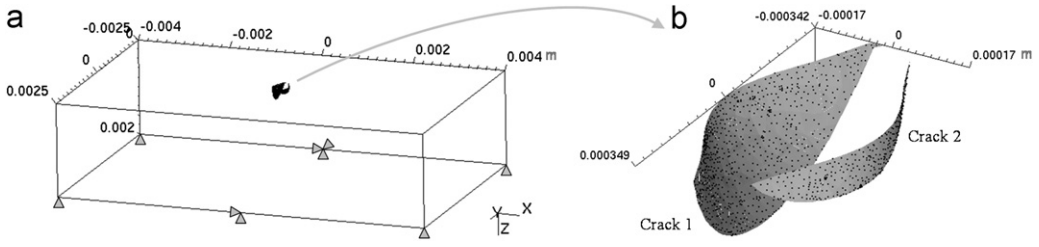

Fig. 13. (a) Geometry of the cracked sample and boundary conditions (m); and (b) 3D crack geometry defined using level-sets based on experimental shapes, and refined crack discretization.

the observations and measurements performed on the metallographic cross-sections (cf. Fig. 3 and Fig. 13(b)). Those actual crack patterns are described with two level set or signed distance functions. Note that the two cracks are defined with only one level set pair (cf. Fig. 14). Crack 1 is 691 μm long on the top surface and 246 μm depth. Crack 2 is 603 μm long and 96 μm depth. The friction coefficient between the crack faces is assumed to be constant and equal to a mean value (μ_C=0.5). The aim here

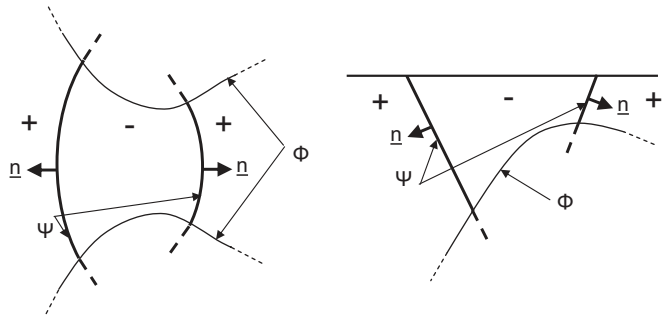

Fig. 14. Definition of crack shape and outward normal for cracks 1 and 2 from the crack level set (Ψ) and the front level set (Φ).

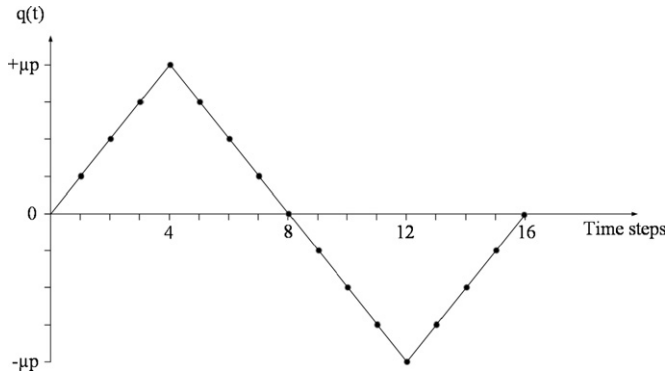

Fig. 15. Cyclic variation of the tangential loading $q(t)$ at each time step of a fretting cycle.

is not to quantify this value but to account for an interface resistance due to several factors (roughness and wear debris among others)

A simplified fretting loading is considered. It consists in a static normal hertzian pressure and a cyclic tangential loading. The normal pressure corresponds to an hertzian pressure p of a 8.4 mm steel ball in flat contact with the top surface of the sample under a constant load $P=80$ N. The radius of contact area is 170 μm. Loading conditions are such that linear elastic assumptions are satisfied. The normalized pressure defined by the ratio of the peak hertzian pressure (1487 MPa) and 1.6 times the yield stress (1200 MPa) is smaller than 1 and equals to 0.775. A cyclic tangential traction $q(t)$ is superimposed and ranges from $-\mu p$ to μp ($\mu=0$, 6). 17 time-steps are considered within one cycle as represented in Fig. 15. A static tensile bulk loading $\sigma_s=200$ MPa is further superimposed.

A finite element mesh of the sample of 21788 tetrahedra is used. The characteristic size of the elements in the crack vicinity is 40 μm. The cracks are discretized with 1095 Gauss points using the refinement algorithm proposed by [23] such as every edge of the interface elements is smaller than 30 μm, cf. Fig. 13(b).

The crack front is defined by the intersection of the iso-zero surfaces of the crack Ψ and front Φ level sets. As only one pair of level sets is considered for the description of cracks 1 and 2, the sign of the crack level set Ψ is negative between the cracks and positive outside. As displayed in Fig. 14, the normal vector of each crack is automatically defined according to the sign of the crack level set [15]. The vector field $[\mathbf{W_T}]$ is hence locally attached to each crack. A given value of $[\mathbf{W_T}]$ for cracks 1 and 2 corresponds to tangential relative displacements of similar magnitudes but of opposite directions with respect to each front local basis.

The approximation of the solution is computed at a level of accuracy of 10^{-4} using the local convergence criterion developed in [25]. An amplified representation of the global displacement field $\mathbf{U}$, the normal and tangential relative displacements $[\mathbf{W_N}]$ and $-[\mathbf{W_T}]$ and the local traction field $\mathbf{T}$ at the crack interface at time steps 0, 4, 8, 12 and 16 are shown in Fig. 15. For convenience, $-[\mathbf{W_T}]$ is plotted instead of $[\mathbf{W_T}]$. The central part between the two cracks is indeed pushed down and experiences a global positive displacement $\mathbf{U}$ according to z global axis (cf. Fig. 13) under the pressure and cracks 1 and 2 experience throughout the fretting cycle $[\mathbf{W_T}]$ negative values expressed in the z global axis.

At time step 0, the tangential traction q is nil. The normal pressure induces tangential relative displacement $[\mathbf{W_T}]$ between cracks 1 and 2 faces whose magnitude is roughly twice and they act in opposite directions (cf. Fig. 16). The local tractions and normal relative displacements between the crack faces are rather small. From time steps 1 to 4, q increases linearly from 0 to its maximum value and is directed from left to right. At time step 4, crack 1 is completely open while crack 2 is closed. $[\mathbf{W_N}]$ and $[\mathbf{W_T}]$ exhibit smooth variations, as well as the traction field between crack 2 faces. $[\mathbf{W_N}]$ reaches maxima values in plane $y=0$. No oscillations are observed. Then, q decreases from qmax to 0 from time steps 4 to 8. Crack 1 closes gradually. From time steps 8 to 12, q drops down to $-$qmax and is directed from right to left. At step 12, crack 1 is completely closed and crack 2 is opened. At the end of the fretting cycle, q is nil again. As cracks 1 and 2 have been opened from tip to mouth during the cycle (at different time steps), hysteresis effects are negligible (time steps 0 and 16).

The refined discretization of the crack interface allows to accurately capture the frictional local contact conditions. It can be noticed that no oscillation of the local fields $\mathbf{W}$ and $\mathbf{T}$ are observed. The proposed model is further able to deal with very small relative displacements between the crack faces $[\mathbf{W}]<2$ μm: 350 times smaller than the length of the crack (≈ 700 μm) and 4000 times smaller than the dimension of the structure (8 mm). This emphasizes once more the need for a multi-scale description of the frictional contact problem between the crack faces and the good properties of the proposed X-FEM model.

The ability of the model to solve complex fracture problems with frictional contact between the crack faces and to account for experimental crack shapes has been demonstrated here. A simplified fretting crack simulation has been performed with the proposed 3D X-FEM model, accounting for 3D experimental complex crack geometries, local contact loading and bulk loading. The frictional contact solution along the crack faces was approximated at a fine scale. This simulation is the first step for more complex and accurate fretting fatigue simulations. Indeed, realistic 3D two-body contact solutions can be obtained using half analytical/FEM external models. Following the work done in 2D by Baietto et al. [38], the results obtained from two-body contact simulations can be used as input loading data for the proposed X-FEM crack growth simulation strategy. Furthermore, experimental crack growth laws dedicated to tribological fatigue problems can also be extracted.

6. Conclusion and perspectives

3D crack pattern characterization and modeling are very challenging tasks. The aim of the work undertaken here is to propose a global approach coupling experiments and numerical modeling to enhance fatigue crack understanding and prediction.

Experimentally, fretting tests have been performed. Fretting crack shapes have been extracted and reconstructed. Those actual crack shapes haven been described with level set functions and are then used as input data for the numerical simulation.

Numerically, an efficient 3D two-scale X-FEM fatigue crack model accounting for frictional contact between the crack faces

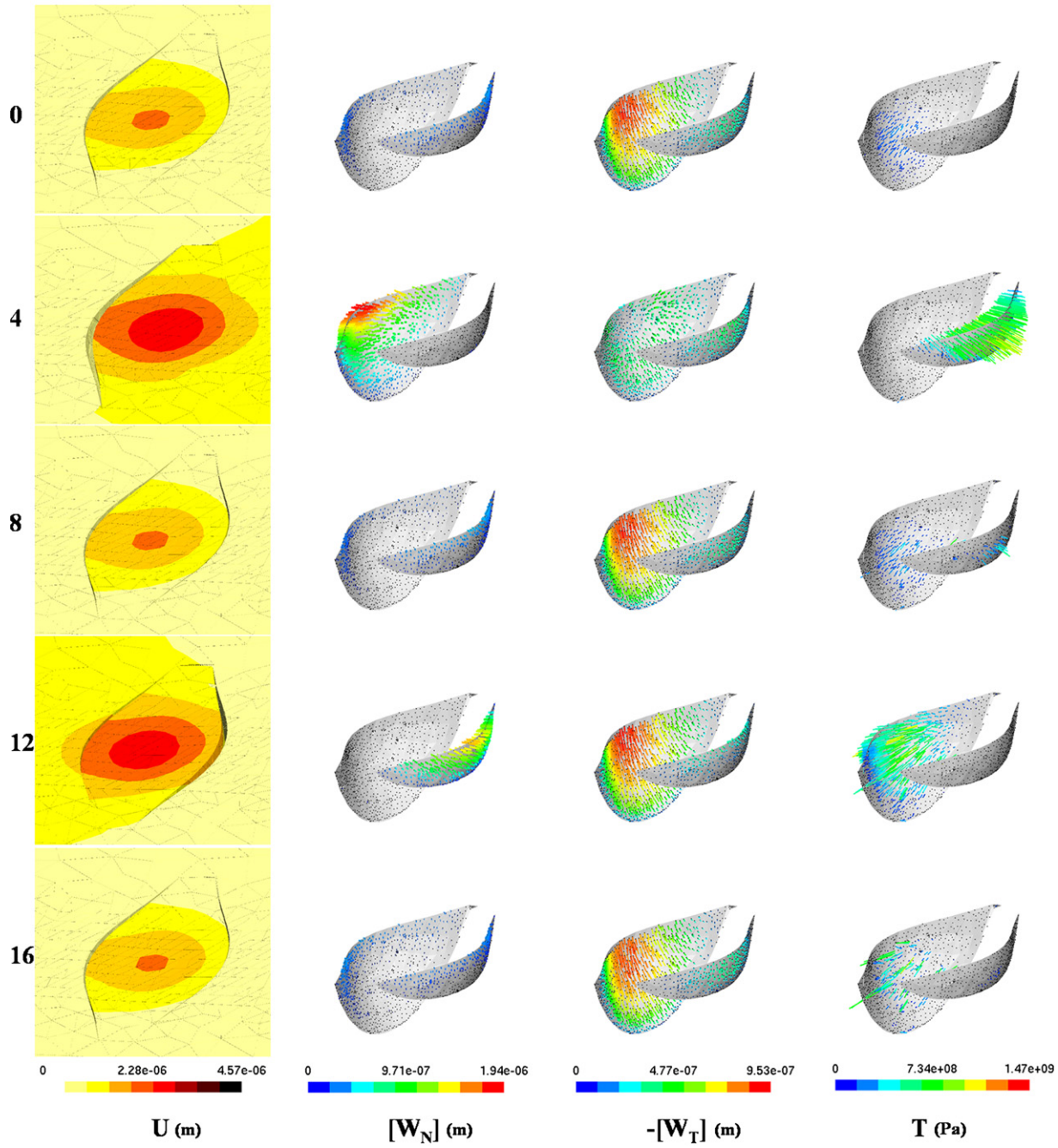

Fig. 16. Amplified representation of the global displacement field **U** (× 10), relative normal displacements [$\mathbf{W_N}$], relative tangential displacements [$\mathbf{W_T}$] and traction field **T** at the interface for time steps 0, 4, 8, 12 and 16.

has been proposed. Its main advantages consist in: a single simple and coarse mesh not conforming the crack is required; neither re-meshing nor field interpolation is needed during the possible crack growth. The proposed three-field weak formulation allows an intrinsic description of the crack interface with a discretization independent from the X-FEM mesh. The refinement of this discretization allows to capture at the pertinent scale the distribution of open and stick-slip contact zones independently of the underlying finite element mesh. Moreover, a specific local convergence criterion has been proposed and a good approximation of the local frictional contact solution is obtained. A wide range of friction coefficients (from 0.2 to 1) can be used. By comparisons between ANSYS results and those obtained from the two-scale X-FEM approach, a very good agreement has been obtained for a given level of accuracy that validates the model.

The simulation of the actual fretting cracks described by a level set pair is then carried out. A simplified fretting test is modeled. Frictional contact conditions are determined during the fretting test. The computation of the stress intensity factors in presence of frictional contact at the crack interface has not been performed here but is under progress.

The next step is to perform such procedure for different number of cycles during the fatigue life to get information on the crack extension and paths. Combining these data with the numerical simulation will allow to propose crack growth laws.

Acknowledgments

The authors are grateful to Ph.D. Student Florent Galland for his help with ANSYS simulations. The support of SKF is also gratefully acknowledged.

References

[1] Vingsbo O, Soderberg D. On fretting maps. Wear 1988;126:131–47.
[2] Vincent L, Berthier Y, Dubourg MC, Godet M. Mechanics and materials in fretting. Wear 1992;153:135–48.
[3] Fouvry S, Kapsa P, Vincent L. Quantification of fretting damage. Wear 1996;200:186–205.
[4] Lamacq V, Dubourg MC. Fretting fatigue crack growth analysis. Experimental photoelastic method combined with numerical method. In: Mechanisms and mechanics of damage and failure, ECF 11; 1996. p. 1387–1392.
[5] Chateauminois A, Kharrat M, Krichen A. Analysis of fretting damage in polymers by means of fretting maps. In: Hoeppner DW, Chandrasekaran V, Elliott CB, editors. Fretting fatigue: current technology and practices, ASTM STP 1367. West Conshohocken, PA: American Society for Testing and Materials; 2000. p. 352–66.
[6] Dubourg MC, Chateauminois A, Villechaise B. In situ analysis and modeling of crack initiation and propagation within model fretting contacts using polymer materials. Tribology International 2003;36:109–19.
[7] Dubourg MC, Lamacq V. Stage II propagation direction under fretting fatigue loading: a new approach in accordance with experimental observations. In: Hoeppner DW, Chandrasekaran V, Elliott CB, editors. Fretting fatigue: current technology and practices, ASTM STP 1367. West Conshohocken, PA: American Society for Testing and Materials; 2000. p. 437–50.
[8] Dubourg MC, Berthier Y, Vincent L. Cracking under fretting fatigue: damage prediction under multiaxial fatigue. Journal of Strain Analysis 2002;37: 519–5336 2002;37:519–33.
[9] Buffière JY, Maire E, Cloetens P, Lormand G, Fougères R. Characterization of internal damage in a MMCp using X-Ray synchrotron phase contrast microtomography. Acta Materialia 1999;47:1613–25.
[10] Cloetens P, Pateyron-Salomé M, Buffière JY, Peix G, Baruchel J, Peyrin F. Observation of microstructure and damage in materials by phase sensitive radiography. Journal of Applied Physics D 1997;81(9):5878–86.
[11] Buffière JY, Proudhon H, Ferrie E, Ludwig W, Maire E, Cloetens P. Three dimensional imaging of damage in structural materials using high resolution micro-tomography. Nuclear Instruments and Methods in Physics Research Section B: Beam Interactions with Materials and Atoms 2005;238:75–82.
[12] Dubourg MC, Villechaise B. Analysis of multiple fatigue cracks. Part I: theory. ASME Journal of Tribololy 1992;114:455–61.
[13] Moës N, Dolbow J, Belytschko. T. A finite element method without remeshing. International Journal for Numerical Methods in Engineering 1999;46:131–50.
[14] Moës N, Gravouil A, Belytschko T. Non-planar 3D crack growth with the extended finite element and level sets—Part 1: mechanical model. International Journal for Numerical Methods in Engineering 2002;53(11):2549–68.
[15] Gravouil A, Moës N, Belytschko T. Non-planar 3D crack growth with the extended finite element and level sets—Part 2: level set update. International Journal for Numerical Methods in Engineering 2002;53(11):2569–86.
[16] Duflot M. A study of the representation of cracks with level sets. International Journal for Numerical Methods in Engineering 2006;70(11):1261–302.
[17] Sukumar N, Chopp DL, Béchet E, Moës N. Three-dimensional non-planar crack growth by a coupled extended finite element and fast marching method. Computer Methods in Applied Mechanics and Engineering 2008;76(5):727–48.
[18] Prabel B, Combescure A, Gravouil A, Marie S. Level set X-FEM non-matching meshes: application to dynamic crack propagation in elastic-plastic media. International Journal for Numerical Methods in Engineering 2006;69:1553–69.
[19] Gravouil A, Elguedj T, Maigre H. An explicit dynamics extended finite element method. Part 2: element-by-element stable-explicit/explicit dynamic scheme. International Journal for Numerical Methods in Engineering 2009;198(30–32):218–2328.
[20] Elguedj T, Gravouil A, Maigre H. An explicit dynamics extended finite element method. Part 1: mass lumping for arbitrary enrichment functions. Journal for Numerical Methods in Engineering 2009;198(30–32):2297–317.
[21] Dolbow J, Moës N, Belytschko T. An extended finite element method for modelling crack growth with frictional contact. Computer Methods in Applied Mechanics and Engineering 2001;53:6825–46.
[22] Vitali E, Benson DJ. Contact with friction in multi-material arbitrary Lagrangian–Eulerian formulations using X-FEM. International Journal for Numerical Methods in Engineering 2008;76(6):893–921.
[23] Giner E, Sukumar N, Denia FD, Fuenmayor FJ. Extended finite element method for fretting fatigue crack propagation. International Journal of Solids and Structures 2008;45(22–23):5675–87.
[24] Liu F, Borja RI. A contact algorithm for frictional crack propagation with the extended finite element method. International Journal for Numerical Methods in Engineering 2008;76(10):1489–512.
[25] Ribeaucourt R, Baietto-Dubourg MC, Gravouil A. A new fatigue frictional contact crack propagation model with the coupled X-FEM/LATIN method. Computer Methods in Applied Mechanics and Engineering 2007;196: 3230–47.
[26] Elguedj T, Gravouil A, Combescure A. A mixed augmented lagrangian extended finite element method for modelling elastic-plastic fatigue crack growth with unilateral contact. International Journal for Numerical Methods in Engineering 2007;71:1569–97.
[27] Géniaut S, Massin P, Moës N. A stable 3D contact formulation for cracks using X-FEM. European Journal of Computational Methods 2007;16:259–76.
[28] Guidault PA, Allix O, Champaney L, Navarro JP. A multiscale computational strategy for crack propagation with local enrichment. Computers and Structures 2007;85(17–18):1360–71.
[29] Rannou J, Gravouil A, Baietto-Dubourg MC. A local multigrid X-FEM strategy for 3-D crack propagation. International Journal for Numerical Methods in Engineering 2008;77:1641–69.
[30] Rannou J, Limodin N, Réthoré J, Gravouil A, Ludwig W, Baietto-Dubourg MC, et al. Three dimensional experimental and numerical multiscale analysis of a fatigue crack. Computer Methods in Applied Mechanics and Engineering 2010;199(21–22):1307–25.
[31] Baietto MC, Rannou J, Gravouil A, Pelletier H, Gauthier C, Schirrer R. 3D crack network analysis during a scratch test of a polymer: a combined experimental and multigrid X-FEM based numerical approach. Tribology International, in press, doi: 10.1016/j.triboint.2010.04.014.
[32] Pierres E, Baietto MC, Gravouil A. A two-scale eXtended Finite Element Method for modeling 3D crack growth with interfacial contact. Computer Methods in Applied Mechanics and Engineering 2010;199(17–20):1165–77.
[33] Ladevèze P. Non-linear computational structural mechanics. New York: Springer; 1998.
[34] Béchet E, Moës N, Wohlmuth B. A stable Lagrange multiplier space for stiff interface conditions within the extended finite element method. International Journal for Numerical Methods in Engineering 2008;78(8):931–54.
[35] Babuska I, Melenk JM. The partition of unity method. International Journal for Numerical Methods in Engineering 1997;40:727–58.
[36] Ferrié E, Buffière JY, Ludwig W, Gravouil A, Edwards L. Fatigue crack propagation: in situ visualization using X-ray microtomography and 3D simulation using the extended finite element method. Acta Materialia 2006;54:1111–22.
[37] Champaney L, Cognard JY, Ladèveze P. Modular analysis of assemblages of three-dimensional structures with unilateral contact conditions. Computers and Structures 1999;73:249–66.
[38] Baietto MC, Pierres E, Gravouil A. A multi-model X-FEM strategy dedicated to frictional crack growth under cyclic fretting fatigue loadings. International Journal of Solids and Structures 2010;47(10):1405–23.